Phosphorus Retention in an Urban Stormwater Pond

Prepared by:

Alina Arvisais

20713478

April 7th, 2021

Supervisor: Dr. Philippe Van Cappellen, University of Waterloo, pvc@uwaterloo.ca

Second Reader: Dr. Mahyar Shafii, University of Waterloo, mshafiih@uwaterloo.ca

This report is submitted as a requirement of BIOL 499 Senior Honours Project.

Acknowledgements

I would like to thank many individuals and groups for their assistance with this project. ICP-OES measurements were conducted by Marianne Vandergriendt and Danielle Green. The Sediment cores were collected by Steph Slowinski, Ari Lisogorsky, Yuba Bhusal, and Bowen Zhou. SEDEX was conducted as a team with Jovana Radosavljevic, Ari Lisogorsky, Yuba Bhusal, and Bowen Zhou, with the guidance of Dr. Shuhuan Li and Dr. Chris Parsons. The flow and water chemistry data for this project has been collected over multiple years by the Ecohydrology Research Group (SPG-Urban team).

I would also like to thank Dr. Philippe Van Cappellen, for taking me on as a BIOL 499 student. Your wisdom, advice, and guidance has been invaluable as I embarked on this learning experience. To Dr. Mahyar Shafii, thank you very much for the feedback you have provided as second reader. Lastly, thank you to Steph Slowinski for your invaluable help. Your passion for the field is inspiring.

Abstract

Stormwater ponds are a critical piece of stormwater infrastructure which were originally developed to reduce local floods associated with the increased impervious surface area of urban environments. They are now increasingly promoted as contaminant sinks preventing downstream export of excess nutrient loads or other contaminants. However, their ability to retain phosphorus (P) and the mechanisms through which retention is achieved are not fully understood. This study investigates the ability of a stormwater pond located in Richmond Hill, Ontario to retain different forms of phosphorus. To evaluate the pond's ability to retain P, sediment cores were collected in different zones of the pond and analyzed for total and operationally defined sediment P pools. To establish a P mass balance for the pond, inlet and outlet water samples collected from 2020-2022 were analyzed for dissolved and particulate P concentrations. The sediment core analyses showed a transition from more reactive to more stable P pools as the sediment aged. The inlet and outlet mass balance results indicate that the pond retains 72% of the inflowing dissolved reactive P (DRP) on an annual basis. This net DRP retention is matched by an increase in the sediment calcium-bound P pool, suggesting that the precipitation of calcium phosphate phases is occurring in the sediments. Because calcium phosphates are effective and stable P sinks, their potential formation in the sediment warrants further study as a P retention mechanism in this urban pond. Overall, the pond retained 70% of the inflowing P, supporting its effectiveness at retaining nutrient P and highlighting the important role of stormwater ponds in stormwater and nutrient management.

Table of Contents

List of Tables v
List of Figures vi
1.0 Introduction 1
2.0 Methods 5
2.1 Study Site 5
2.2 Sediment Sample Collection and Preservation 5
2.3 Solid-phase Organic Carbon 6
2.4 HCl-extractable P and Other Elements 6
2.5 Sequential Extractions of Sediment P Pools (SEDEX) 7
2.6 Inlet and Outlet Water Flow and Chemistry Data 8
2.7 Mass Balance Approach 8
2.7.1: Burial Flux Estimation 9
2.7.2: Inlet and Outlet Flux Estimation 10
3.0 Results 12
3.1 HCl-Extractable P (TP) 12
3.2 SEDEX 13
3.3 Mass Balance Approach 15
3.3.1 Atmospheric Deposition Flux 16
3.3.2 Burial Flux 16
3.3.4 Inlet and Outlet Flux and Retention 17
4.0 Discussion 19
4.1 Mass Balance Agreement 19
4.2 P Burial Trends in the Pond Sediment 20
4.3 Proposed P Retention Mechanism 21
5.0 Conclusion 24
6.0 Future Directions 25
7.0 References 26
Appendix A 31

List of Tables

Table 1: Retention of TP, TDP, and DRP..... 17

Table 2: Calculated Annual Fluxes of TP, TDP, and DRP at the Inlet and Outlet..... 18

List of Figures

Figure 1: Side-profile of a stormwater pond 2

Figure 2: Sediment Core Locations 5

Figure 3: Aerial View of the Stormwater Pond 10

Figure 4: Total Phoshprus (TP) Extraction Results for Each Sediment Core 12

Figure 5: Total Phosphorus: Total Aluminium (TP: Total Al) Ratio for Each Sediment Core 13

Figure 6: SEDEX Extraction Results 14

Figure 7 Yearly Total P Budget for the Stormwater Pond 15

Figure 8 Yearly Total P Retained, Yearly Surface Area Normalized P Retained, and Sediment Mass Deposited for Each Pond Region. 17

Figure A1. Organic Carbon Content of Pond Sediment Cores 31

Figure A2. Aluminium (Al) Content of Pond Sediment Cores 32

Figure A3. Iron (Fe) Content of Pond Sediment Cores 33

Figure A4. Manganese (Mn) Content of Pond Sediment Cores 34

Figure A5. Sulphur (S) Content of Pond Sediment Cores 35

Figure A6. SEDEX Results: Absolute P Value 36

Figure A7. SEDEX Results: Absolute P Value Without Inlet Suspended Sediment 36

1.0 Introduction

Stormwater management ponds—or stormwater ponds for short—are small ponds situated downstream of a developed catchment, but upstream of receiving waters (Frost et al., 2019). As a critical piece of stormwater infrastructure, they were originally designed with flow reduction as the main goal, given the local flooding that occurs because of the increased impervious surface area of urban catchments (Lusk & Chapman, 2021). However, they are now increasingly promoted as contaminant sinks for preventing downstream export of excess nutrient loads or other contaminants (Taguchi et al., 2020).

The role of stormwater ponds as a nutrient sink is important because human activities in urban catchments result in considerable emissions of nutrients which cause eutrophication in downstream water bodies (Carey et al., 2013). Phosphorus (P) especially is a key urban derived nutrient in stormwater (Carey et al., 2013). In fact, in many freshwater bodies, P has been identified as the limiting nutrient to algal activity and therefore excess P is often considered to be the primary cause of algal blooms and water quality deterioration (Schindler et al., 2016; Schindler et al., 1978). As such, the ability of stormwater ponds to retain P and mitigate P delivery downstream is particularly relevant.

Stormwater ponds have been found to have highly variable P retention efficiencies, ranging from 10-90% (Frost et al., 2019). But more generally, P retention is quite low at about 30-40% (Frost et al., 2019). Stormwater ponds are primarily designed to remove, and thus retain, contaminants, including P, is by particle sedimentation and physical adsorption (Pettersson et al., 1999). The design of stormwater ponds promotes these removal mechanisms by: (1) having a

physically separated forebay section, (2) an extended water retention time, and (3) a high sediment surface area to pond volume ratio (shallow depth). These design characteristics influence pond function in a few ways. The shallow depth allows for a well-mixed water column that keeps the sediment surface oxygenated (Austin et al., 2021). This is meant to deter Fe or Al-bound P from being released from the sediment (Lusk & Chapman, 2021). However, hypoxia at the sediment-water interface can alter the redox conditions and result in P release (Lusk & Chapman, 2021). The extended water retention time allows increased settling time for particulate phosphorus (Frost et al., 2019). Lastly, the separated forebay serves as a specialized settling basin for incoming stormwater runoff (Song et al., 2017). In this way, both the extended water retention time and forebay serve to increase sedimentation. However, P sedimentation is limited by the fact that the water column P is split between dissolved P, which does not settle, and particulate P, which can settle (Frost et al., 2019).

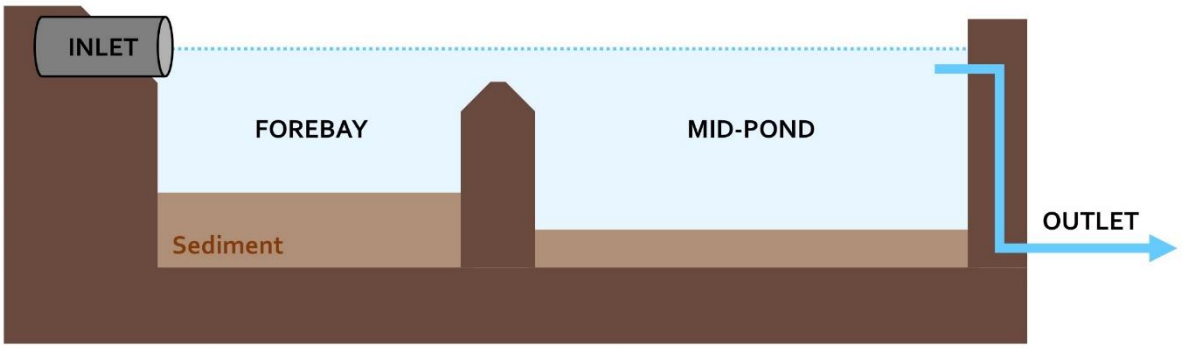

Figure 1: Side-profile of a stormwater pond. Note the separated forebay which acts as a settling basin.

P may also be removed from the pond through uptake by resident biota (Frost et al., 2019). However, subsequent sedimentation of organic matter contributes to the pool of labile

organic P found in the sediment (Song et al., 2017). Organic P has been shown to be readily released from the sediment to the water column regardless of oxygenation levels in the pond (Song et al., 2017). This means sediment organic P may allow for temporary storage but could also fuel internal loading in the long-term (Song et al., 2017; Taguchi et al, 2020). Especially during the summer season, when biological activity, extracellular enzymatic activity, and fast mineralization of organic P is high (Song et al., 2017; Taguchi et al, 2020). Consequently, the sediment organic P fails to act as a permanent sink.

Overall, more biogeochemically dynamic elements such as P exists in many forms each with different reactivity and bioavailability, leading to more complex removal and burial processes (Frost et al., 2019). Owing to these more complex processes, instead of permanently retaining P, stormwater ponds appear to modify urban derived P by reducing the amount of one form and increasing the amount of another through phosphorus cycling in the pond (Song et al., 2015).

To further investigate P retention in stormwater ponds, an urban stormwater pond located in Richmond Hill, Ontario was studied. In studying this pond, the objective is to evaluate the pond's ability to retain P. Two approaches were employed to achieve this goal: (1) sediment cores obtained from different zones of the pond were used to reconstruct a history of long-term P retention in the pond; (2) a mass balance approach was used to calculate the annual retention efficiency of the pond. Using two types of extractions, the sediment cores were used to measure the total P content and P distribution across 6 operationally defined pools. To establish a P mass balance for the pond, inlet and outlet water samples collected from 2020-2022 were analyzed for dissolved and particulate P concentrations. These two approaches are used together to shed light

on how P is transformed both as it flows through the pond and as the sediment ages. This will provide more information on the possible P retention mechanisms of the pond.

2.0 Methods

2.1 Study Site

The study site is a stormwater management pond built in 1998 and currently overseen by the City of Richmond Hill (Facility 19-8). The pond is located in Richmond Hill, Ontario off Elgin Mills Road, at the end of Melbourne Drive and was built at the outlet of a 10.45-hectare residential catchment. The pond was dredged in 2006, after which three sediment surveys were conducted in July of 2007, June of 2012, and June of 2016.

2.2 Sediment Sample Collection and Preservation

To evaluate how the sediment P pools varied spatially in the pond, sediment cores were collected from four different zones of the pond: the inlet-Forebay, the middle of the main pond basin, near the outlet of the main pond basin, and the bank of the main pond basin near the vegetation on the shore.

Figure 2: Sediment Core Locations

The cores were collected on February 24th, 2021, using a Universal Percussion Corer (Aquatic Research Instruments, Hope, ID). The forebay core was 29.0 cm long, the mid-pond core was 8.5 cm long, the bank core was 8.0 cm long, and the outlet core was 9.0 cm long. Within 36 hours of sampling, the cores were sectioned into 1cm intervals. Each core section was placed in a Whirl Pack bag and frozen at -20 ºC before being freeze-drying. Following freeze-drying, the sediment was ground using a mortar and pestle and sieved to <125 µm using a stainless steal sieve.

2.3 Solid-phase Organic Carbon

Organic carbon (C) was analyzed for by combustion analysis at 550 °C using an Elementar vario EL cube analyzer. Samples were prepared for analysis by weighing approximately 30 mg of (freeze-dried, ground and sieved) sediment into tin wraps. The detection limit for organic C was 1%. Sulfanilamide was used as an internal standard material for data correction, and its organic C content was measured with 10% error.

2.4 HCl-extractable P and Other Elements

To extract the total sediment phosphorus (P), aluminium (Al), manganese (Mn), iron (Fe), and sulphur (S), the method by Aspila et al., (1976) was followed. To do so, 1 mL of 100% wt/wt magnesium nitrate was added to 0.1 g of freeze-dried sediment. These were ashed at 550°C in a muffle furnace for 2 hours. Next, the ashed sediment was resuspended in 10 mL of 1M HCl and incubated for 16 hours before filtering through a 0.45 µm pore size nylon membrane filter. These extracts were diluted 1:10 in a 2% nitric acid matrix and analyzed by

ICP-OES (Thermo Scientific iCAP 6,000) for P, aluminum (Al), manganese (Mn), iron (Fe), and sulfur (S). The method detection limit (MDL) for the elements in the soil for the analysis of the extract by ICP-OES were 0.05, 3.4, 0.19, 1.2, and 3.9 µmol/g for sediment Al, Mn, Fe, S, and Na respectively.

2.5 Sequential Extractions of Sediment P Pools (SEDEX)

The sediment core samples were extract using a sequential extraction (SEDEX) method developed by Ruttenberg (1992) with an added extraction step following the method presented by Baldwin (1996) to extract P associated with humic and fulvic acids. This method extracts six operationally defined pools in the following order: the easily exchangeable (P_{Ex}, 1 M $MgCl_2$), humic-bound (P_{Hum}, 1 M$NaHCO_3$), redox labile (P_{Fe}, CDB), carbonate- and/or fluorapatite-bound (P_{CFA}, 1M acetate, pH 4), detrital apatite and/or other inorganic P (P_{Detr}, 1M HCl), and organic (P_{Org}, ashing at 550degC then 1 M HCl) P pools using the extractants 1 M magnesium chloride ($MgCl_2$), 1 M sodium bicarbonate ($NaHCO_3$), citrate-dithionite (CDB), 1 M acetate at pH 4, 1 M HCl, and 1 M HCl after ashing at 550 ºC, respectively. The added 1 M $NaHCO_3$ extraction step from Baldwin (1996) is used to extract for the P associated with humic substances. This “humic-bound” P pool would otherwise be extracted during the extraction with 1 M CDB for the redox- labile P pool, which represents P associated with Fe and Mn oxides and oxyhydroxides. This adapted SEDEX method has been used by others before, e.g., O’Connell et al. (2020) and Parsons et al. (2017).

A 0.1g sediment sample was used for the sequential extractions, which were conducted in the manifold system developed by Ruttenberg (2009). Each sample was extracted in duplicate. Each extract obtained was diluted 1:10 in a 2% nitric acid matrix and the total dissolved P

concentrations of the diluted extracts were measured by inductively coupled plasma optical emission spectrometry (ICP-OES; Thermo Scientific iCAP 6,000). Matrix-matched standards were analyzed for each sequential extraction reagent to evaluate and correct for matrix effects.

2.6 Inlet and Outlet Water Flow and Chemistry Data

To analyze the input and output of the pond, a dataset of flow and water chemistry data collected by the Ecohydrology Research Group (ERG) at the University of Waterloo was used. This data set contains measurements from fall 2020 to winter 2022. Level data was collected at the inlet and the outlet of the pond using level loggers (Teledyne ISCO Area Velocity Flow Logger), and level data was converted to flow using a rating curve. Water samples were collected during rainfall and snowmelt events using ISCO samplers (Teledyne ISCO 6712 Portable Samplers) and were analyzed for three different phosphorus pools: total phosphorus (TP), total dissolved phosphorus (TDP), and dissolved reactive phosphorus (DRP). TP was determined by according to the acid persulfate digestion method from Dayton et al. (2017), coupled with detection by ICP-OES (Thermo Scientific iCAP 6,000). TDP was determined by filtering the water samples with a <0.45 μm, and again the phosphorus content was measured using ICP-OES. Lastly, DRP was determined as per the colorimetric molybdenum blue method described by Ringuet et al. (2011).

2.7 Mass Balance Approach

Four different fluxes of P into and out of the pond water column were identified: inlet flux, atmospheric deposition flux, burial flux, and outlet flux. Different methods were applied to

estimate values for each of these. The atmospheric deposition flux was identified by using the surface area of the pond and a literature search of area normalized atmospheric deposition rates for regions near the field site. The methods used to estimate the burial, inlet, and outlet fluxes are described below.

2.7.1: Burial Flux Estimation

The sediment levels of the pond were surveyed by the City of Richmond Hill in 2007, 2012, and 2016. Based on this data, the pond was separated into boxes 6.34m wide, to match with the distance between the points surveyed along the transect. Numeric integration of the sediment profile data was then used to determine the accumulated sediment profile height for each box. Next, Google Earth was used to measure the surface area of each box (Google Earth Pro, 2018.). Based on the surface area and sediment profile height, the volume of sediment deposited into each box between 2007 and 2016 was determined. The bulk density of the sediment was estimated based on the average organic carbon content of the sediment (Appendix A) and the correlation between bulk density and organic carbon reported by Avnimelech et al. (2001). The estimated bulk density of 0.427 g/cm^3, was used to convert sediment volume to sediment mass. Lastly, the pond was separated into three distinct regions: the forebay (0-25.35 m from the inlet), main basin (25.35-57.03 m from the inlet), and the outlet (57.03-69.70 m from the inlet). For each of these regions, the average HCl-extractable P per gram of sediment for their

respective sediment core(s) was used to calculate the amount of P deposited in the sediment for the 2007-2016 period.

Figure 3: Aerial View of the Stormwater Pond

Figure 3 above is an aerial view of the stormwater pond, overlayed with the boxes it was separated into. The purple boxes represent the forebay, the orange boxes represent the main basin, and the yellow boxes represent the outlet.

2.7.2: Inlet and Outlet Flux Estimation

The average inlet and outlet concentration of DRP, TDP, and TP were determined. The average concentrations (C) at the inlet and outlet were used to estimate the retention ratio of the pond for each P pool as follows:

$$Retention = \frac{C_{avg_{in}} - C_{avg_{out}}}{C_{avg_{in}}}$$

To estimate the annual flux at the inlet, the following formula was applied:

$$Flux_{inlet} = C_{avg_{in}} \cdot Q_{avg_{in}} \cdot N_s$$

Where Q is the average discharge (flow) for all measurements at the inlet, and N_s is the number of seconds in a year.

To estimate the flux at the outlet, the following formula was applied:

$$Flux_{outlet} = Flux_{inlet} \cdot Retention$$

An assumption of this approach is that the average flow into and out of the pond are equal on an annual basis. This assumption may not be true due to water losses through evapotranspiration and/or groundwater recharge (Anderson et al., 2015).

3.0 Results

3.1 HCl-Extractable P (TP)

The results of the total phosphorus (TP) extraction for each 1 cm interval sample of each core are presented in figure 4 below. As a note, these cores are representative of sediment P accumulation since the pond was last dredged during 2006. As such, this represents sediment P accumulation over a relatively short period of time (14 years).

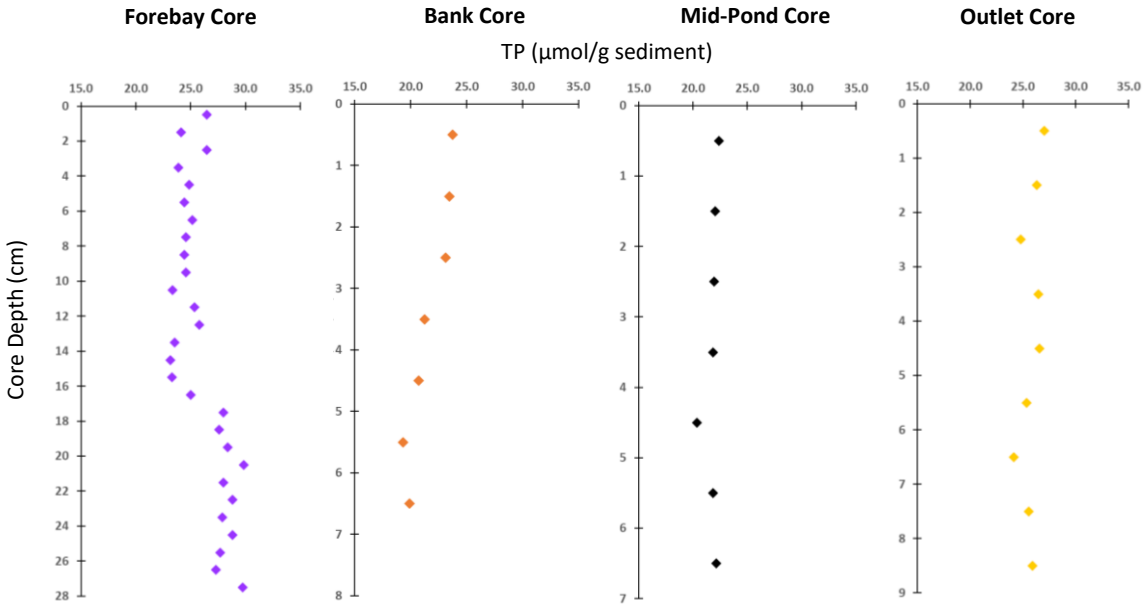

Figure 4: Total Phoshprus (TP) Extraction Results for Each Sediment Core

The TP concentration for most cores has remained relatively constant over the depth of the sediment (figure 4). However, these different regions of the pond have slightly different amounts of TP; the forebay and outlet cores have higher TP amounts than the bank and mid-pond core.

When the TP content of each sample is normalized to the Al content for each respective sample, a trend of slowly increasing TP over decreased core depth is observed, as shown in

figure 5 below. The normalization to Al is used since Al is an indicator of conservative catchment weathering.

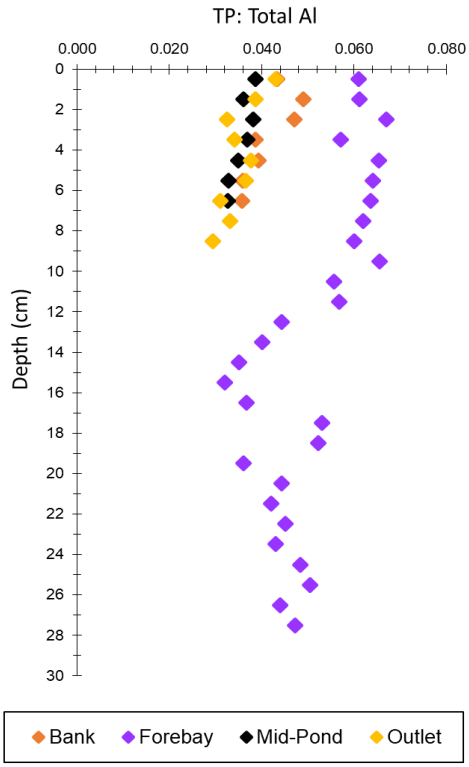

Figure 5: Total Phosphorus: Total Aluminium (TP: Total Al) Ratio for Each Sediment Core

The total P to total Al ratio increases up the core (figure 5). There is also a higher total P to total Al ratio in the forebay compared to the rest of the pond. This indicates that consistently higher levels of P are being retained in the forebay sediment than in the rest of the pond.

3.2 SEDEX

The SEDEX method was used for its ability to differentiate between six different sediment P pools. Of these six pools, four of them are considered more reactive, while two are considered more stable. Easily exchangeable, humic-bound, iron-bound, and organic P are the

four more reactive and bio-available pools. While calcium-bound and detrital P are relatively stable sediment P pools.

Due to the involved nature of the method, six samples were chosen for this analysis. This included three forebay samples (5-6 cm, 12-13 cm, 21-22 cm), one bank sample (3-4 cm), one mid-pond sample (3-4 cm), and one outlet sample (3-4cm). These were chosen to visualize P pool distribution along the length of the forebay core, as well as to compare the P pool distribution at the same depth for the other core. In addition to the six sediment core samples, one sample of suspended sediment collected at the inlet on November 11, 2020 was used.

Figure 6 below shows the relative distribution of the six P pools for selected sediment samples.

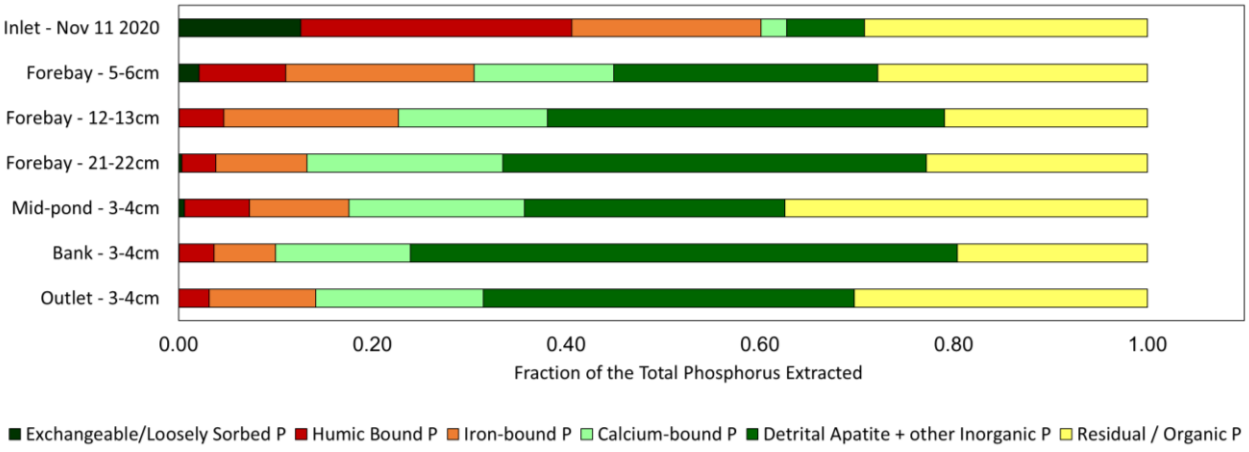

Figure 6: SEDEX Extraction Result. The abundance of the six P pools is represented as the fraction of the total phosphorus extracted.

The inlet suspended sediment sample is mostly composed of exchangeable, humic-bound, and iron-bound P, which are reactive (figure 6). Comparing the inlet suspended sample to the most up-core pond sediment samples, the proportion of these three reactive P pools is decreased

(figure 5). This indicates that as P enters the pond and is buried in the pond sediment, there is a transformation of P from more reactive phases to more stable ones as P.

Additionally, as the depth of the forebay core increases, the proportion of these reactive P pools continues to decrease, such that at a depth of 21-22 cm the total P is primarily composed of calcium-bound and detrital P (figure 5). Thus, as the sediment of the pond ages there is a growing dominance of more stable P pools.

3.3 Mass Balance Approach

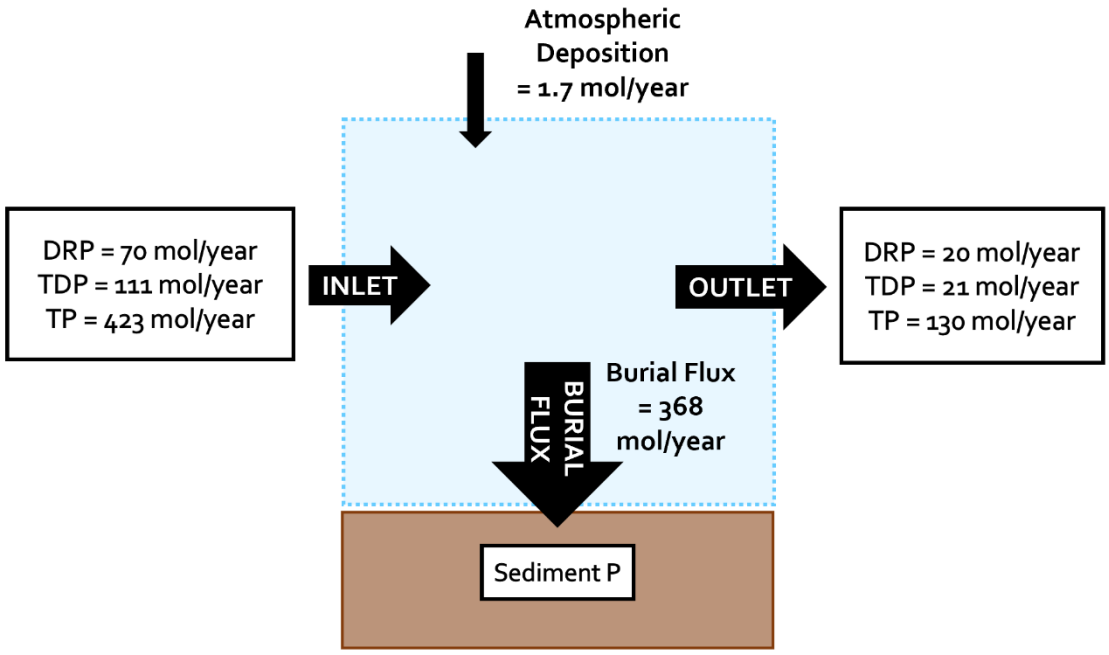

Figure 7 Yearly Total P Budget for the Stormwater Pond.

Figure 7 above is a diagrammatic representation of the total P budget of the pond, for the 2021 year. The atmospheric deposition flux is 1.7 mol P/year. The inlet flux of total P is 427 mol/year, while the outlet P flux is 130 mol/year. Finally, the burial flux was estimated to be 368 mol/year.

3.3.1 Atmospheric Deposition Flux

From the literature, an atmospheric deposition rate of P of 0.26 kg/ha/year was selected to represent the atmospheric deposition to the surface of the stormwater pond. This rate was calculated from the mean atmospheric load of P to the surface of Lake Simcoe over the 2002-2007 period (Scott et al., 2006; Lake Simcoe Region Conservation Authority, 2009). This rate was selected from the literature since it represents the observed atmospheric deposition for the site located most closely to the stormwater pond.

Multiplying this rate by the Google Earth determined surface area of the pond (2051 m^2), the total phosphorus load to the pond from atmospheric deposition is 1.7 mol P/yr. This is the smallest contributor of P to the pond.

3.3.2 Burial Flux

The burial flux represents the net deposition flux of phosphorus into the sediment. It depends both on P retention in the sediment and P release from the sediment to the water column. The total estimated value of the burial flux is 368 mol/year. Of this 368 mol/year retained in the sediment across the pond, 227 mol/year is retained in the forebay region, 105 mol/year in the main basin, and 36 mol/year near the outlet (Figure 8). Of these regions, the main basin has the largest surface area (996 m^2), then the forebay (884 m^2), and the outlet (171 m^2). Additionally, the forebay retained 9.3 tonnes/year of sediment, while the main basin retained 4.8 tonnes/year, and the outlet region retained 1.4 tonnes/year (Figure 8).

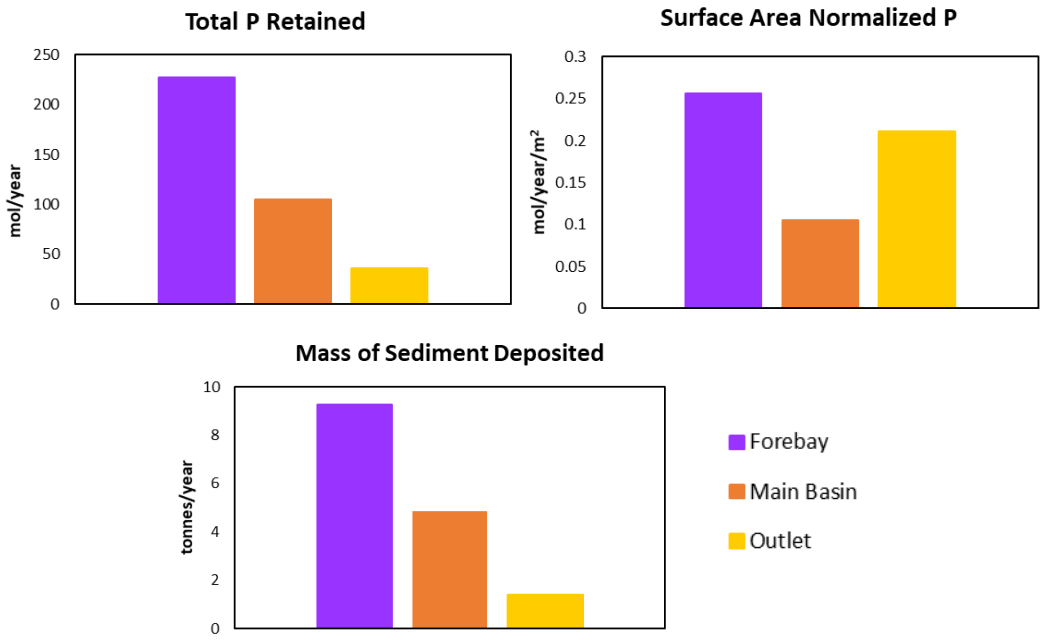

Figure 8 Yearly Total P Retained, Yearly Surface Area Normalized P Retained, and Sediment Mass Deposited for Each Pond Region.

3.3.4 Inlet and Outlet Flux and Retention

The average concentration of TP, TDP, and DRP of water flowing at the inlet and outlet is presented in table 3.3.4.1 below.

Table 1: Retention of TP, TDP, and DRP

	C_{TP} (µmol/year)	C_{TDP} (µmol/year)	C_{DRP} (µmol/year)
Inlet	7.9	2.1	1.3
Outlet	2.4	0.40	0.37
Retention (%)	70	81	72

Based on the average concentration at the inlet and outlet of the pond, the pond has a high retention ratio for each of TP, TDP, and DRP.

Looking more closely at the DRP at the inlet and outlet, the DRP:TP ratio decreases from 0.17 at the inlet, to 0.15 at the outlet. Indicating that the pond also decreases the proportion of this most reactive dissolved P pool as water flows through.

The average inlet flow was determined to be 1.71 L/s. This was used in calculating the estimated fluxes in to and out of the pond, which are presented in table 3.3.4.2 below.

Table 2: Calculated Annual Fluxes of TP, TDP, and DRP at the Inlet and Outlet.

	TP	TDP	DRP
Inlet Flux (mol/year)	423	111	70
Outlet (mol/year)	130	21	20

As in Table 2, the inlet flux of total P into the pond is 423 mol/year, while the outlet flux of total P from the pond is 130 mol/year. This would mean, that with the atmospheric deposition flux, 295 mol P/year is retained in the pond. This is on the same order of magnitude as the burial flux which was estimated to be 358 mol/year.

4.0 Discussion

4.1 Mass Balance Agreement

The final P budget for the pond is represented in figure 3.3. As expected, atmospheric loading is a very small contributor to the pond's P budget at an input of 1.7 mol/year. The inlet flux of TP was determined to be 427 mol/year. This can be compared to the TP export coefficient for another nearby residential catchment. For the southern areas of the Lake Simcoe watershed (roughly 50 km from the Richmond Hill study site), a report was contracted by the Ontario Ministry of the Environment. This report determined the P export coefficient for the residential area to be 1.32 kg/ha/year (Hutchinson Environmental Sciences Ltd., 2012). Based on this export coefficient, the estimated expected load to the pond is 445 mol/year (10.45 ha catchment area). This compares well to calculated inlet TP flux. Finally, the burial flux was estimated to be 358 mol/year. Since, according to the P budget, the burial flux should also represent the difference between the inlet flux, outlet flux, and atmospheric deposition flux it is useful to compare these. The difference between these three fluxes is 295 mol/year, which agrees quite well with the calculated burial flux (358 mol/year). Altogether, this suggests that the final P budget is well-balanced.

Discrepancies may be due in part to the difference in the timescale represented by the calculated burial flux and the calculated inlet and outlet fluxes. Because the sediment TP represents TP accumulation since 2007, the burial flux represents the average burial flux over the last 14 years. However, the inlet and outlet fluxes are based on approximately one year of data from the end of 2020 to early 2022. Therefore, the inlet and outlet fluxes are subject to yearly variability in flow and P loading to the pond. Additionally, due to some gaps in the flow data

which have not yet been resolved, flow-weighted, ratio, and regression estimators could not be used to more formally established the value of the inlet and outlet fluxes. Despite this, these more crudely determined values agree with the burial flux (calculated independently) and the expected load from the catchment. Though it would be valuable to gap-fill the flow record and apply methods such as flow-weighted averaging and the Beale ratio estimator.

Lastly, the pond showed much higher retention (70% for TP) than a reported average for stormwater ponds (30-50%) (Frost et al., 2019; Taguchi et al., 2020). While this is not outside the range of P retention observed in ponds, it does raise questions about the potential mechanism that allows for this observation.

4.2 P Burial Trends in the Pond Sediment

Observing the quantity and type of P retained in the sediment is useful since it allows for the visualization of long-term trends of P retention. In this case, the sediment record of the pond represents the physical and chemical environment of the pond over approximately the last 14 years.

The TP trends, when normalized to Al as in figure 3.1.2, show a slight increase in TP as core depth decreases. They also highlight the consistently higher TP: Total Al ratio for the forebay, which is indicative of a more highly P enriched sediment. This is consistent with the expectation that P-rich inflowing suspended sediment is likely to settle and accumulate in this zone of the pond. This is also supported by the increased sediment retention in the forebay, measuring at 9.3 tonnes/year of sediment compared to the main basin at 4.8 tonnes/year despite

its smaller surface area. This suggests that the forebay is effective at slowing the inflowing stormwater and allowing P-rich sediment to settle at an increased rate.

When comparing deeper sediment samples to suspended sediment and core segments close to the surface, inferences can be made about the different transformations of P that are occurring in the pond. The SEDEX results display a general transition from more to less reactive sediment P as suspended sediment enters the pond and settles, and as the pond sediment ages. Notably, the proportion of reactive P represents about 10% of the total P in the suspended sediment entering the pond but is barely present in the pond sediment. Similarly, humic-bound P and Fe-bound P also decrease in proportion. Opposite to this, the proportion of Ca-bound P increases and so does detrital P. This is different to what has been reported in literature for stormwater ponds, where the sediment appeared to be mostly composed of organic P (Song et al., 2017). In the ponds where this is observed, the labile organic P fuels internal loading and limits P retention in the pond (Taguchi et al., 2020). Thus, the dominance of stable P pools in this pond makes it unique, as does its high retention efficiency (70-80%). This suggests there may be some mechanism(s) that is leading to these results both in P retention and P transformation.

4.3 Proposed P Retention Mechanism

Considering the movement from less stable to more stable P pools as the sediment ages, generally this could be that the more reactive P is lost to the water column through internal loading. But the high P retention of the pond suggests otherwise. Therefore, there must be a mechanism that allows for the retention of P in more stable sedimentary pools.

The pond was also observed to decrease the DRP:TP ratio from the inlet (0.17) to the outlet (0.15). With retention efficiency for DRP measured at 72%, this suggests that reactive P is being sequestered in the pond. Additionally, while the TP content remains relatively similar across the forebay core (Figure 3.1.1), the net Ca-bound P concentration increases down the core. These observations point to the formation of calcium phosphate mineral phases as a retention mechanism.

Much like P, Ca concentrations are found to be enriched in urban areas (Wu et al., 2018). In the case of Ca, it is enriched primarily from the weathering of ageing cement and other construction materials (Wu et al., 2018). In natural water bodies, Ca is an important factor which controls the concentration of DRP, wherein DRP reacts with Ca to form calcium phosphate mineral phases (Wu et al., 2018). Calcium phosphate minerals are stable P sinks which are not likely to dissolve once formed (Kraal et al., 2017). The hypothesis that DRP is being retained by the in situ precipitation of calcium phosphate mineral phases is further supported by comparing the annual retention flux of DRP and the burial flux of Ca-bound P. The annual DRP retention flux was calculated as the difference between the inlet and outlet DRP fluxes. The burial flux of Ca-bound P was determined using the same method as the TP burial flux but substituting the average Ca-bound P concentration in the sediment. Doing so, gives 50 mol/year of retained DRP and 59 mol/year of buried Ca-bound P. These numbers agree quite well.

However, the interaction between P and Ca is dependent on many environmental factors such as pH, salinity, and concentration of P and Ca (House, 2010). Therefore, the chemical environment of the pond should be simulated using specialized software such as PHREEQC to determine the likelihood of calcium phosphate mineral formation. Additionally, using methods

such as SEM, TEM, and XRD, the presence of calcium phosphate minerals in the sediment should be confirmed (Oxmann & Schwendenmann, 2014).

5.0 Conclusion

To summarize the conclusions of this research, the pond shows high retention of P (70-80%). This is above the literature reported average P retention efficiency of 30-40%, but not beyond the observed range of 10-90%. The stormwater pond also transformed the inflowing P from more reactive to less reactive forms. This is evident by the decrease in the DRP:TP ratio from the inlet to the outlet of the pond. As well as by the SEDEX results, which show a reduction in the proportion of the 4 reactive P pools, and an increase in the proportion of the 2 stable P pools. The high retention of P, and more specifically DRP, as well as the transformation to more stable P phases suggests that there is an effective P sink for DRP in the pond. The results so far point to this possibly being Ca-bound P via the formation of calcium phosphate mineral phases. Their potential formation in the sediment warrants further study as a P retention mechanism in this urban pond. Overall, these findings highlight the important role of stormwater ponds in stormwater and nutrient management.

6.0 Future Directions

Going forward, next steps in the project include:

1. Further investigation of Ca-bound P as a potential sink for DRP in the pond. This would include simulating the chemical environment of the pond to determine whether it is thermodynamically favourable to the formation of calcium phosphate mineral phases. As well as using methods such as SEM, TEM, and electron diffraction to observe the presence of amorphous calcium phosphate mineral phases in the sediment.
2. Applying well-developed flux estimation methods to the inlet and outlet data. This would first require gap-filling of the flow data, then applying estimators such as flow-weighted averaging, the Beale ratio estimator, and a Fergusson regression.
3. Conducting SEDEX on some of the top sediment core samples (i.e. 0-1cm) and more inlet and outlet suspended sediment samples. This would provide a more representative view of the incoming and outflowing suspended sediment in the pond. The top sediment core sample would also provide more information about the P composition of freshly deposited sediment before it ages.

7.0 References

Anderson, M. P., Woessner, W. W., & Hunt, R. J. (2015). Spatial Discretization and Parameter Assignment. In Applied Groundwater Modeling (pp. 181–255). Elsevier. https://doi.org/10.1016/b978-0-08-091638-5.00005-5

Austin, D., Liao, H., & Scharf, R. (2021). Phosphorus solubilization in stormwater ponds: rapid field assessment to identify ponds with excessive total phosphorus concentrations. In Environmental Science: Water Research & Technology (Vol. 7, Issue 12, pp. 2346–2356). Royal Society of Chemistry (RSC). https://doi.org/10.1039/d1ew00413a

Aspila, K. I., Agemian, H., & Chau, A. S. Y. (1976). A semi-automated method for the determination of inorganic, organic and total phosphate in sediments. The Analyst, 101(1200), 187. https://doi.org/10.1039/an9760100187

Avnimelech, Y., Ritvo, G., Meijer, L. E., & Kochba, M. (2001). Water content, organic carbon and dry bulk density in flooded sediments. In Aquacultural Engineering (Vol. 25, Issue 1, pp. 25–33). Elsevier BV. https://doi.org/10.1016/s0144-8609(01)00068-1

Baldwin, D. S. (1996). The phosphorus composition of a diverse series of Australian sediments. Hydrobiologia, 335(1), 63–73. https://doi.org/10.1007/bf00013684

Carey, R. O., Hochmuth, G. J., Martinez, C. J., Boyer, T. H., Dukes, M. D., Toor, G. S., & Cisar, J. L. (2013). Evaluating nutrient impacts in urban watersheds: Challenges and research opportunities. In Environmental Pollution (Vol. 173, pp. 138–149). Elsevier BV. https://doi.org/10.1016/j.envpol.2012.10.004

Dayton, E. A., Whitacre, S., & Holloman, C. (2017). Comparison of three persulfate digestion methods for total phosphorus analysis and estimation of suspended sediments. In Applied Geochemistry (Vol. 78, pp. 357–362). Elsevier BV. https://doi.org/10.1016/j.apgeochem.2017.01.011

Frost, P. C., Prater, C., Scott, A. B., Song, K., & Xenopoulos, M. A. (2019). Mobility and Bioavailability of Sediment Phosphorus in Urban Stormwater Ponds. Water Resources Research, 55(5), 3680–3688. https://doi.org/10.1029/2018wr023419

Google Earth Pro version 7.3. (July 5, 2018). *Richmond Hill Stormwater Pond, ON Canada. 43°53'24.22" N 79°24'08.49" W,* eye alt 493m. <http://www.google.com/earth/index.html > (Accessed October 25, 2021).

House, W. A. (1999). The Physico-Chemical Conditions for the Precipitation of Phosphate with Calcium. In Environmental Technology (Vol. 20, Issue 7, pp. 727–733). Informa UK Limited. https://doi.org/10.1080/09593332008616867

Hutchinson Environmental Sciences Ltd. (2012). *Phosphorus Budget Tool in Support of Sustainable Development for the Lake Simcoe Watershed*. https://www.aurora.ca/en/business-and-development/resources/Environment-and-Sustainability/Phosphorus-Budget-Guidance-Verison-2-1.pdf

Kraal, P., Dijkstra, N., Behrends, T., & Slomp, C. P. (2017). Phosphorus burial in sediments of the sulfidic deep Black Sea: Key roles for adsorption by calcium carbonate and apatite authigenesis. In Geochimica et Cosmochimica Acta (Vol. 204, pp. 140–158). Elsevier BV. https://doi.org/10.1016/j.gca.2017.01.042

Lusk, M. G., & Chapman, K. (2021). Chemical Fractionation of Sediment Phosphorus in Residential Urban Stormwater Ponds in Florida, USA. In Urban Science (Vol. 5, Issue 4, p. 81). MDPI AG. https://doi.org/10.3390/urbansci5040081

O'Connell, D. W., Ansems, N., Kukkadapu, R. K., Jaisi, D., Orihel, D. M., Cade-Menun, B. J., Hu, Y., Wiklund, J., Hall, R. I., Chessell, H., Behrends, T., & Van Cappellen, P. (2020). Changes in Sedimentary Phosphorus Burial Following Artificial Eutrophication of Lake 227, Experimental Lakes Area, Ontario, Canada. In Journal of Geophysical Research: Biogeosciences (Vol. 125, Issue 8). American Geophysical Union (AGU). https://doi.org/10.1029/2020jg005713

Oxmann, J. F., & Schwendenmann, L. (2014). Quantification of octacalcium phosphate, authigenic apatite and detrital apatite in coastal sediments using differential dissolution and standard addition. Copernicus GmbH. https://doi.org/10.5194/osd-11-293-2014

Parsons, C. T., Rezanezhad, F., O'Connell, D. W., & Van Cappellen, P. (2017). Sediment phosphorus speciation and mobility under dynamic redox conditions. In Biogeosciences (Vol. 14, Issue 14, pp. 3585–3602). Copernicus GmbH. https://doi.org/10.5194/bg-14-3585-2017

Pettersson, Thomas & German, J. & Svensson, G. (1999). Pollutant removal efficiency in two stormwater ponds in Sweden. Doktorsavhandlingar vid Chalmers Tekniska Hogskola. 866-873.

Ringuet, S., Sassano, L., & Johnson, Z. I. (2011). A suite of microplate reader-based colorimetric methods to quantify ammonium, nitrate, orthophosphate and silicate concentrations for

aquatic nutrient monitoring. In J. Environ. Monit. (Vol. 13, Issue 2, pp. 370–376). Royal Society of Chemistry (RSC). https://doi.org/10.1039/c0em00290a

Ruttenberg, K. C. (1992). Development of a sequential extraction method for different forms of phosphorus in marine sediments. Limnology and Oceanography, 37(7), 1460–1482. https://doi.org/10.4319/lo.1992.37.7.1460

Ruttenberg, K. C., Ogawa, N. O., Tamburini, F., Briggs, R. A., Colasacco, N. D., & Joyce, E. (2009). Improved, high-throughput approach for phosphorus speciation in natural sediments via the SEDEX sequential extraction method. Limnology and Oceanography: Methods, 7(5), 319–333. https://doi.org/10.4319/lom.2009.7.319

Scott LD, Winter JG, Girard RE. 2006. Annual water balances, total phosphorus budgets, and total nitrogen and chloride loads for Lake Simcoe (1998-2004). Lake Simcoe Environmental Management Strategy Implementation Phase III Technical Report No. Imp. A.6. Lake Simcoe Region Conservation Authority, Newmarket, Ontario, Canada

Schindler, D. W., Carpenter, S. R., Chapra, S. C., Hecky, R. E., & Orihel, D. M. (2016). Reducing Phosphorus to Curb Lake Eutrophication is a Success. In Environmental Science & Technology (Vol. 50, Issue 17, pp. 8923–8929). American Chemical Society (ACS). https://doi.org/10.1021/acs.est.6b02204

Schindler, D. W., Fee, E. J., & Ruszczynski, T. (1978). Phosphorus Input and Its Consequences for Phytoplankton Standing Crop and Production in the Experimental Lakes Area and in Similar Lakes. In Journal of the Fisheries Research Board of Canada (Vol. 35, Issue 2, pp. 190–196). Canadian Science Publishing. https://doi.org/10.1139/f78-031

Song, K., Winters, C., Xenopoulos, M. A., Marsalek, J., & Frost, P. C. (2017). Phosphorus cycling in urban aquatic ecosystems: connecting biological processes and water chemistry to sediment P fractions in urban stormwater management ponds. Biogeochemistry, 132(1–2), 203–212. https://doi.org/10.1007/s10533-017-0293-1

Song, K., Xenopoulos, M. A., Marsalek, J., & Frost, P. C. (2015). The fingerprints of urban nutrients: dynamics of phosphorus speciation in water flowing through developed landscapes. Biogeochemistry, 125(1), 1–10. https://doi.org/10.1007/s10533-015-0114-3

Taguchi, V. J., Olsen, T. A., Natarajan, P., Janke, B. D., Gulliver, J. S., Finlay, J. C., & Stefan, H. G. (2020). Internal loading in stormwater ponds as a phosphorus source to downstream waters. In Limnology and Oceanography Letters (Vol. 5, Issue 4, pp. 322–330). Wiley. https://doi.org/10.1002/lol2.10155

Wu, P., Yin, A., Fan, M., Wu, J., Yang, X., Zhang, H., & Gao, C. (2018). Phosphorus dynamics influenced by anthropogenic calcium in an urban stream flowing along an increasing urbanization gradient. In Landscape and Urban Planning (Vol. 177, pp. 1–9). Elsevier BV. https://doi.org/10.1016/j.landurbplan.2018.04.005

Appendix A

Supplementary Material

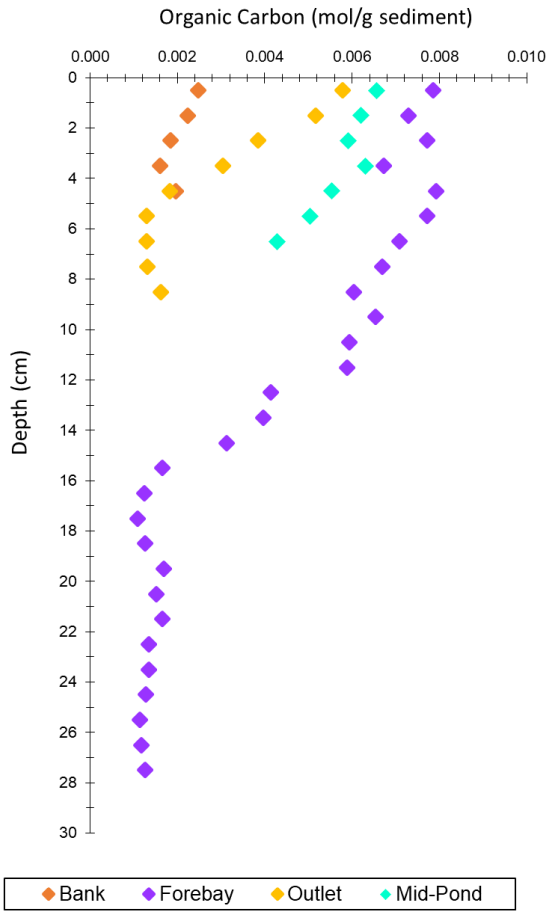

Figure A1. Organic Carbon Content of Pond Sediment Cores

The average organic carbon content of the sediment is 0.0036 mol/g sediment (43.66 mg/g sediment).

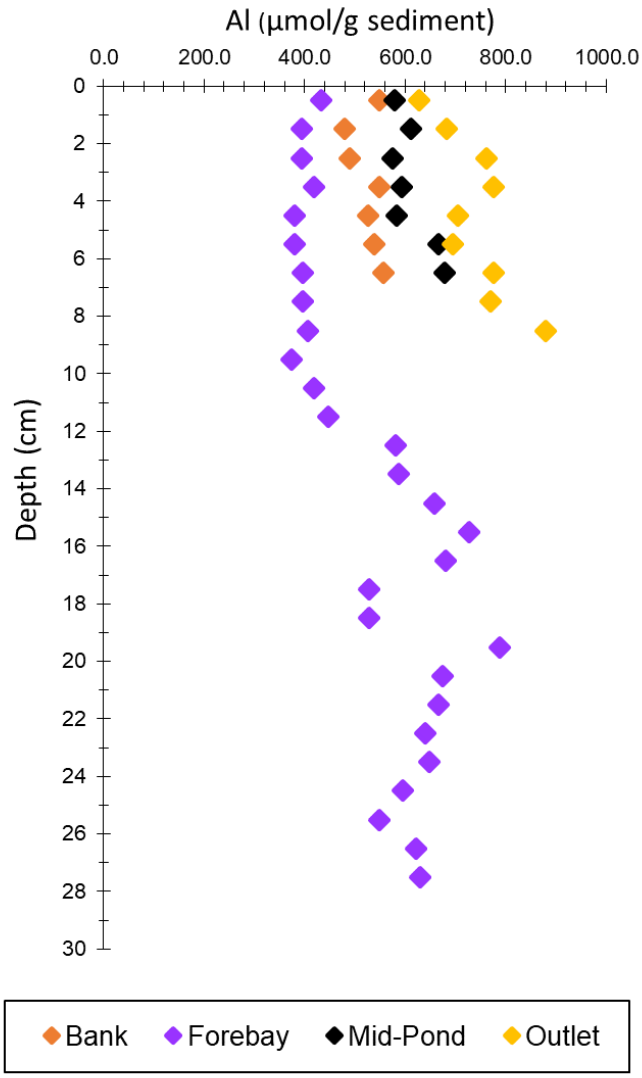

Figure A2. Aluminium (Al) Content of Pond Sediment Cores

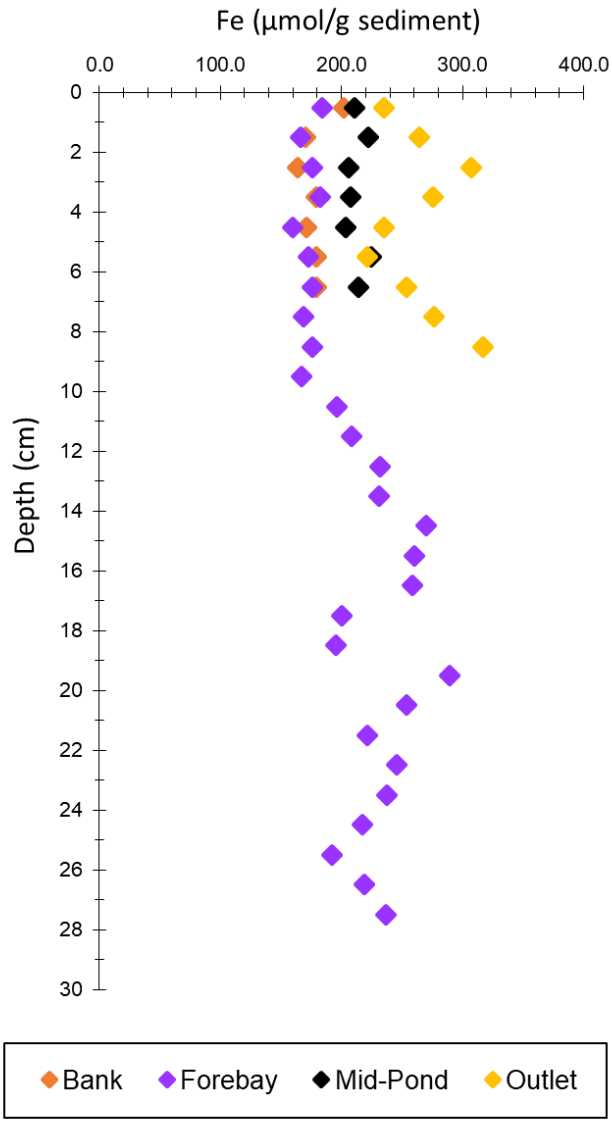

Figure A3. Iron (Fe) Content of Pond Sediment Cores

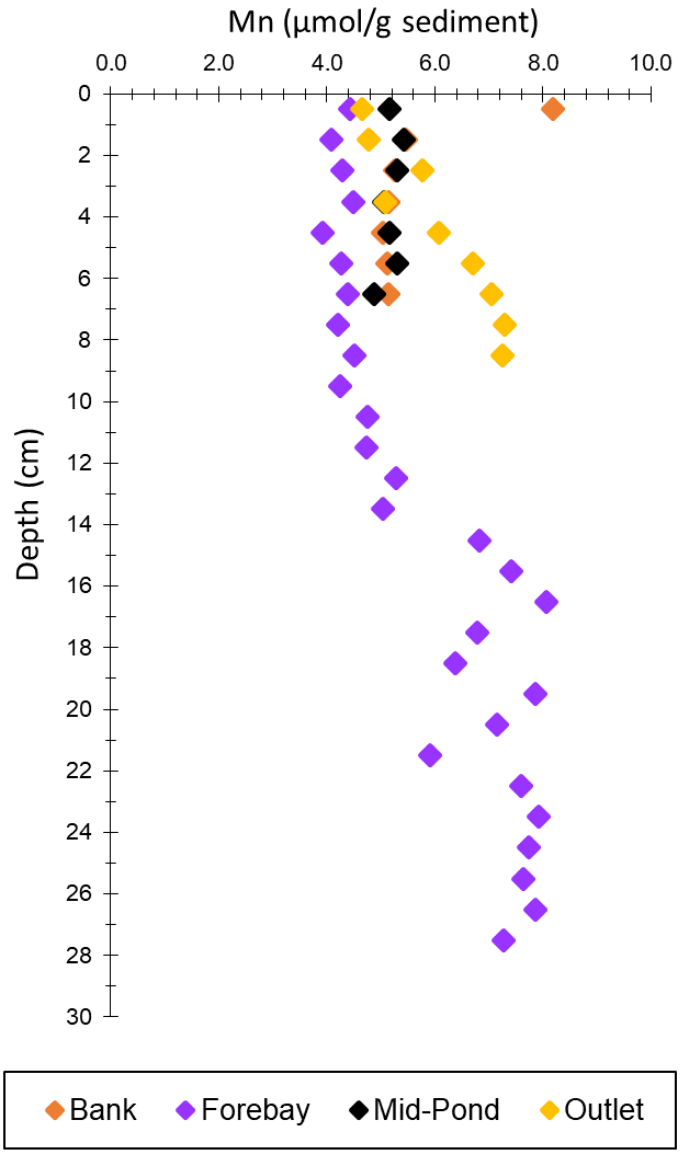

Figure A4. Manganese (Mn) Content of Pond Sediment Cores

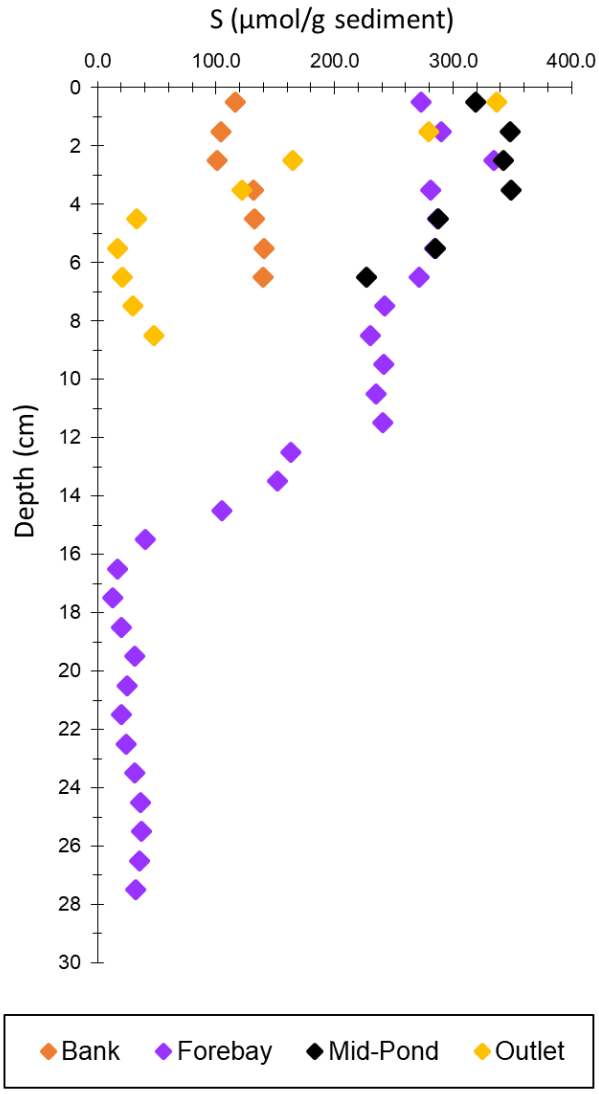

Figure A5. Sulphur (S) Content of Pond Sediment Cores

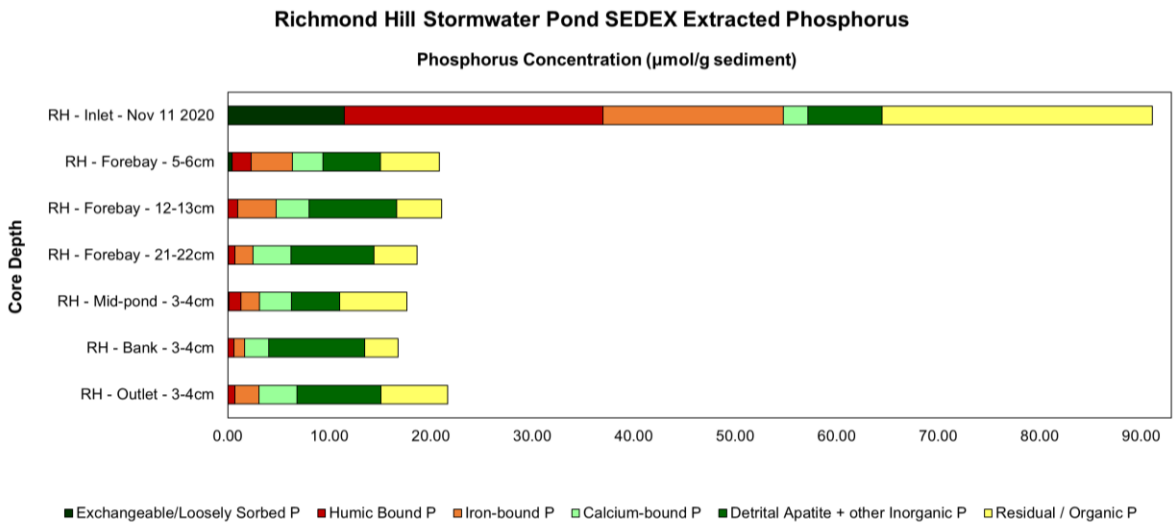

Figure A6. SEDEX Results: Absolute P Value

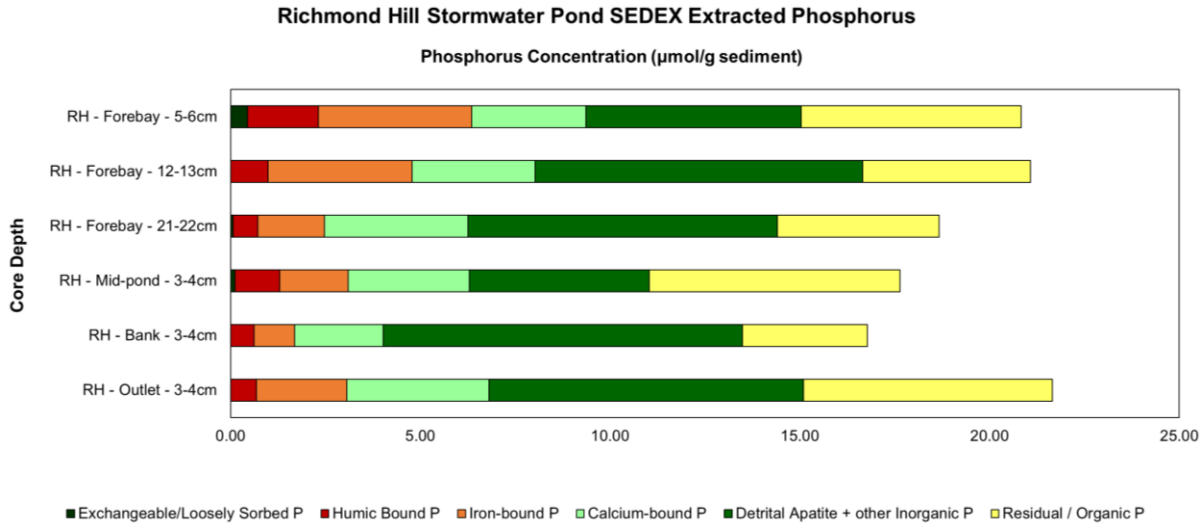

Figure A7. SEDEX Results: Absolute P Value Without Inlet Suspended Sediment